



Palladium-catalyzed 1,3-butadiene telomerization with methanol. Improved catalyst performance using bis-*o*-methoxy substituted triarylphosphines

John R. Briggs^a, Henk Hagen^b, Samir Julka^a, Jasson T. Patton^{a,*}

^aThe Dow Chemical Company, Corporate R&D, 1776 Building, Lab D-5, Midland, MI 48674, USA

^bDow Benelux B.V., Herbert H. Dowweg 5, P.O. Box 48, 4530 AA Terneuzen, The Netherlands

ARTICLE INFO

Article history:

Received 1 December 2010

Received in revised form

3 February 2011

Accepted 7 February 2011

Keywords:

1,3-Butadiene

Telomerization

Electrospray ionization-mass spectrometry (ESI-MS)

1-Methoxy-2,7-octadiene

1-Octene

ABSTRACT

New, improved phosphine ligands for palladium-catalyzed butadiene telomerization with methanol have been discovered. Using high throughput experimentation and an Electrospray Ionization-Mass Spectrometry (ESI-MS) investigation of telomerization catalysts solutions, we have identified phosphines of the type $P(C_6H_4-2-OMe)_2(C_6H_5-n(X)_n)$, where X is an electron-withdrawing group, as high selectivity, high activity phosphine ligands for butadiene telomerization with methanol to 1-methoxy-2,7-octadiene (MOD-1). These ligands were designed to mitigate anaerobic oxidation of phosphines by alkylation which was shown by Electrospray Ionization-Mass Spectrometry (ESI-MS) studies to correlate with catalyst death and palladium precipitation in working telomerization catalyst solutions. The best phosphine-promoted catalysts achieve selectivities to desired 1-methoxy-2,7-octadiene of 94% at high butadiene conversion, significantly improved over those achieved commercially by triphenylphosphine.

© 2011 Elsevier B.V. All rights reserved.

1. Introduction

A number of different transition metals have been reported to catalyze the telomerization of conjugated dienes, but the most active appears to be palladium [1]. Since the initial reports of its performance [2], the palladium-catalyzed telomerization of 1,3-dienes with nucleophiles has become a popular area of research. The telomerization of 1,3-butadiene with a nucleophile such as methanol or water has been of particular interest due to the commercial significance of the resulting products [3]. Ligand promoters for the palladium-catalyzed reaction include phosphines [4], isonitriles [5], and N-heterocyclic carbenes [6]. A large variety of phosphines have been reported to be effective ligands for palladium telomerization catalysts, but only a limited study of the structure-performance correlations has been undertaken [7]. The mechanism of palladium-catalyzed butadiene telomerization has been examined by Keim [8], Jolly [9], and Beller [10]. The critical step required to form methoxy-terminated telomers, carbon-oxygen bond formation, is proposed to occur either by intra- or intermolecular nucleophilic attack by methanol or methoxide on a π -allyl complex derived from a C_8 hydrocarbyl ligand that is formed by the oxidative coupling of two butadiene molecules at palladium (Fig. 1).

The commercially desired product of the palladium-catalyzed telomerization of 1,3-butadiene with methanol is 1-methoxy-2,7-octadiene (MOD-1, **1**), (Fig. 1). A significant use of this material is its ultimate conversion to 1-octene, a monomer in great demand for a variety of polyolefin applications. In recent years, The Dow Chemical Company has sought performance improvements in order to consider commercial production of 1-octene from butadiene [11]. The first step in this process is the telomerization of butadiene with methanol using a homogeneous triphenylphosphine-promoted palladium catalyst with a sodium methoxide promoter to enhance the reaction rate. The most significant by-products of this reaction are 3-methoxy-1,7-octadiene (MOD-3, **2**) and 1,3,7-octatriene (**3**) (Fig. 2).

Increased conversions and greater selectivity to **1** would increase the throughput of the commercial plant and give better raw material efficiency. While significant improvements in selectivity have been reported in the literature using N-heterocyclic carbenes as ligands for palladium telomerization catalysts, the N-heterocyclic carbene ligands are costly, and the resulting catalysts require high concentrations of base promoter for their optimal performance (typically 1 mol % base relative to butadiene). Economic constraints generally favor the retrofit of an improved catalyst into the existing plant, since any new catalyst is required to perform under conditions that are fully compatible with the existing plant configuration, hardware, and catalyst handling procedures.

* Corresponding author. Tel.: +1 989 636 1978; fax: +1 989 638 6225.

E-mail address: jpatton@dow.com (J.T. Patton).

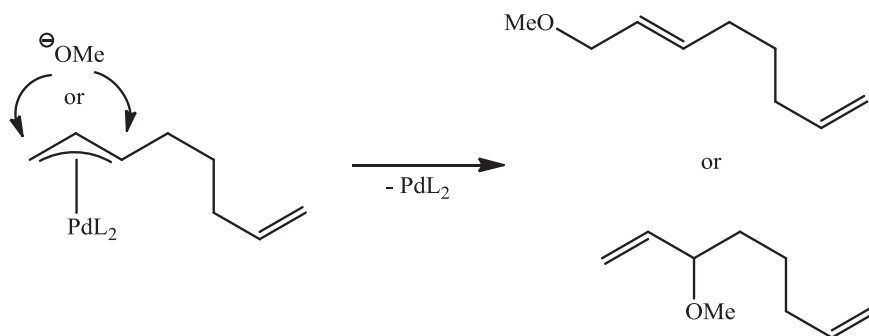


Fig. 1. Proposed intermolecular nucleophilic attack by methanol or methoxide on a palladium π -allyl complex.

In this study, we have focused our efforts on developing a more selective monodentate triarylphosphine ligand to improve catalyst performance that would more likely operate within the constraints of the existing commercial plant. High-throughput experimentation was utilized on different ligands as depicted in Fig. 3. In addition, Electrospray Ionization-Mass Spectrometry (ESI-MS) investigation was carried out on telomerization catalysts solutions to understand the role of ligand basicity in palladium-catalyzed telomerization reactions.

2. Results and discussion

2.1. High throughput catalyst screening

While a number of studies indicate a considerable influence of the phosphine ligand on the performance of palladium catalysts during butadiene telomerization, a thorough understanding of the effect of the phosphine structure on catalyst performance has not appeared in the literature [4]. We began this study to improve catalyst performance using high throughput (HTP) methodology to investigate a diverse library of monodentate-phosphine ligands looking for improvements in either selectivity to **1** or catalyst productivity. The general approach and equipment used was similar to that reported previously from this laboratory [12]. Selected results of our initial HTP experiments that examined some 50 ligands under a number of reaction conditions are shown in Table 1. Plots of this data in Fig. 4 show the selectivity to **1** and total productivity of a series which includes “isosteric” *para*-substituted triarylphosphines as a function of Tolman’s ligand electronic parameter (Chi values) [13]. This set of ligands was included in the experimental design so that we might explore catalyst performance as a function of ligand electronic properties in the absence of concurrent changes in ligand steric properties. Nevertheless, the complete HTP library included sterically and electronically diverse ligand structures and was undertaken as a means to identify promising ligand classes for further study. A class of ligands that performed particularly well was 2-methoxyaryl phosphines, as they exhibited both high selectivity and catalyst productivity under the HTP conditions.

The plots in Fig. 4 show a strong correlation between catalyst productivity and selectivity to **1** with the Tolman ligand Chi value, with more basic ligands (lower Chi) performing better. Both

selectivity and productivity, expressed as turnover number in moles of **1** per moles of palladium in a 2 h reaction, are higher at 5.0 M initial methanol concentration than at 2.0 M methanol. Interestingly, data for tris(2-methoxyphenyl)phosphine, **L8**, appears to fall on the same lines as the isosteric 4-substituted triarylphosphines, suggesting there may be little steric effect manifested with this phosphine in this reaction. However, the data for tris-(2,4,6-trimethoxyphenyl) phosphine, **L9**, (not shown in Fig. 3) do not correlate well with the rest of the data, and for this ligand, steric effects (Chi = -8.1, cone angle = 184°) may well be at play. Significantly, both selectivity and productivity are maximized at low ligand Chi and at the higher methanol concentration for **L1–L8**. Under these experimental conditions the benchmark triphenylphosphine-promoted catalyst (**L4**) demonstrated only moderate productivity of 1232 g **1**/g Pd, and a selectivity of only 74% to **1**. All catalysts promoted by triarylphosphines with electron-releasing *para*-substituents exceeded the performance of the triphenylphosphine-promoted catalyst in both selectivity and productivity. Not only was the catalyst system derived from **L8** the most productive, but it gave among the highest selectivities observed (93% to **1**), making it one of the most selective phosphine-promoted catalysts reported to date. The very basic and sterically encumbered tris(2,4,6-trimethoxyphenyl)phosphine also performed very well under these conditions, although, in contrast to the other ligands listed in Table 1, its performance decreased at higher methanol concentration.

Although high throughput (HTP) experimentation offers dramatic increases in experimental productivity, it also suffers from some limitations. To fully capture the experimental productivity increases that HTP experimentation offers, reagent and product transfer is achieved robotically, preferably by syringing liquids and solutions. With volatile substrates, however, such as butadiene, this procedure limits the concentration that can be effectively added without encountering losses due to expulsion of liquid contents from the robotic syringes due to the high vapor pressure of such volatile reagents. We found that we could reproducibly syringe solutions of butadiene in methylcyclohexane solvent at concentrations no greater than 2 M, which gave a concentration of butadiene in the reactor of only about 1 M after dilution with the required minimum amount of methanol. This butadiene concentration is significantly lower than that employed in the commercial telomerization process. Additionally, because of reactor volume limitations of the HTP

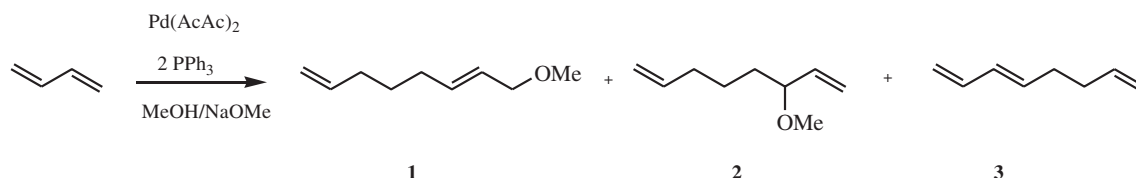


Fig. 2. Major products of triphenylphosphine/palladium-catalyzed 1,3-butadiene telomerization with methanol.

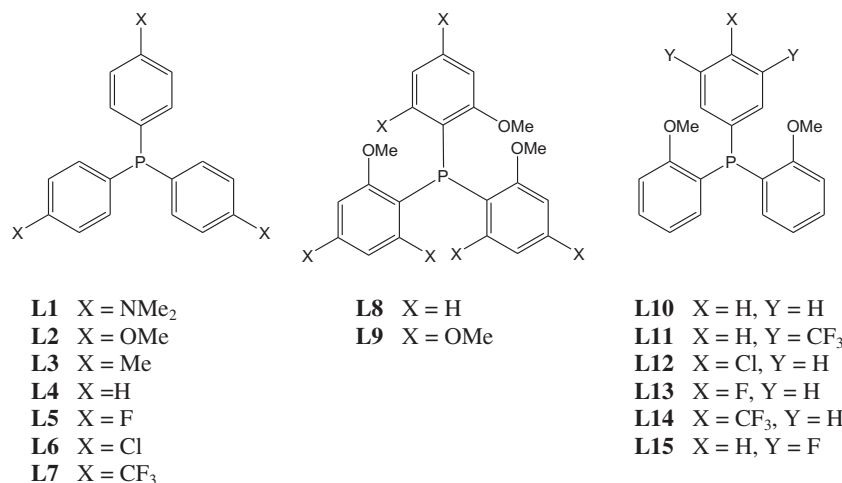


Fig. 3. Substituted triarylphosphines examined.

equipment initial methanol concentrations of 2.0 and 5.0 M were used in these experiments. Furthermore, a palladium concentration of 3.2×10^{-4} M (40 ppm), somewhat higher than that used commercially, was employed to ensure that the catalysts were not unduly affected by catalyst poisons. These choices resulted in the maximum turnover numbers achievable by the catalyst in these HTP experiments being ca. 1660, which is much lower than that which is required commercially. Having employed high throughput experimentation to expediently identify the better-performing ligands, we turned our efforts to examining the performance of the most promising ligands under more relevant conditions (i.e. at higher initial methanol (12.7 M) and butadiene (2.5 M) concentrations, and lower palladium concentrations 7.7×10^{-5} M (10.9 ppm), and at a higher temperature of 90 °C). These conditions forced us to employ a different experimental procedure using a Fischer-Porter bottle which allowed us to work at similar concentrations used commercially. To our surprise, under these new conditions, the most basic ligands which had performed so well under the high throughput conditions now performed poorly, exhibiting profoundly depressed productivities. This data is shown in Table 2.

The relationship of the ligand basicity, quantified by plotting the catalysts TON values versus ligand Chi values under the reaction conditions employed commercially is shown in Fig. 5. The increasing activity with decreasing ligand Chi value seen at 5.0 M methanol and 1.0 M butadiene concentrations is not seen under these conditions. Of particular note was the dramatic decline in the performance of the catalyst promoted by ligand **L2**. Under these conditions, the catalyst promoted by this ligand exhibited poor activity while maintaining good MOD-1 selectivity.

2.2. Decomposition of phosphines during telomerization

Phosphonium salts have been reported as promoters for telomerization catalysts by Kuraray [15] suggesting that such species play a significant role in the phosphine telomerization catalyst solutions. Indeed, Behr has suggested that phosphonium salts may be acting as a reservoir of free ligand in telomerization catalysts [3]. Additionally, in studies of the telomerization of isoprene using palladium catalysts promoted by the very bulky and very basic phosphine tris(2,4,6-trimethoxyphenyl)phosphine, a phosphonium salt of this type has been isolated when the reaction is performed in the absence of other nucleophiles [16]. Based on this earlier work which had shown that phosphine ligands can be alkylated to give phosphonium cations during the telomerization

reaction through a mechanism that mirrors a step in the formation of the desired reaction product, **1**, we sought to determine if this process was involved in the early loss of catalyst activity when using the more basic phosphines. It is well known that phosphines are competent nucleophiles and they have been shown to react with metal π -allyls [17]. Thus, we sought to confirm that phosphine ligands were being converted to phosphonium cations of the type $[\text{Ar}_3\text{PCH}_2\text{CH}=\text{CHCH}_2\text{CH}_2\text{CH}_2\text{CH}=\text{CH}_2]^+$ under telomerization conditions, and determine if this process could be related to the loss of catalytic activity observed with the more basic ligands at higher methanol concentrations. It is known that such phosphonium salts can be solvolysed in basic alcoholic media to phosphine oxides [18], which we had previously seen in catalyst solutions after the reaction, although we could not rule out aerobic oxidation as an explanation for their formation.

Table 1

Performance data of selected triarylphosphines for butadiene telomerization obtained from high throughput studies.

Ligand	Substituent	Chi ¹³ (χ)	[MeOH] _{initial} (M/l)	TON (mol / mol Pd)	Selectivity to 1 (mol %)
L1	4-NMe ₂	5.6	2	898	76
			5	1224	87
L2	4-OMe	10.2	2	554	57
			5	1143	83
L3	4-Me	10.5	2	259	38
			5	1012	81
L4	4-H	12.9	2	138	23
			5	933	74
L5	4-F	15	2	33	16
			5	560	60
L6	4-Cl	16.8	2	5	11
			5	409	51
L7	4-CF ₃	20.6	2	0	NA
			5	91	48
L8	2-OMe	2.7	2	1145	87
			5	1342	93
L9	2,4,6-(OMe) ₃	-8.1 ^a	2	1264	94
			5	862	93

Conditions: [Pd] = 3.2×10^{-4} M (40 ppm), [NaOMe] = 1.6×10^{-3} L/Pd = 2, T = 80 °C, [butadiene]_{initial} = 1.0 M, reaction time = 2 h. Methylcyclohexane was added to each reactor to equalize the total reaction volume (5.0 mL). Productivity and selectivity values are averages of two runs, except in cases where one value was suspect. In these cases, the data from the higher productivity run is reported. Maximum TON for 100% yield of **1** is 1660. NA – not applicable.

^a Value for **L9** was estimated from a value of $v(\text{CO})$ for $[\text{Ni}(\text{CO})_3\text{L}]$ [14].

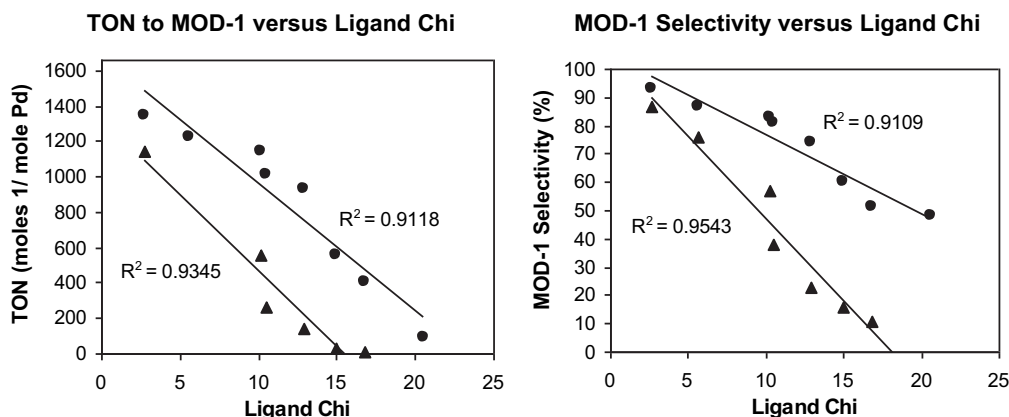


Fig. 4. Plots of selectivity and productivity to **1** for ligands shown in Table 1 (**L9** excluded). ● – $[\text{MeOH}]_{\text{initial}} = 5.0 \text{ M}$; ▲ – $[\text{MeOH}]_{\text{initial}} = 2.0 \text{ M}$; $[\text{Pd}] = 3.2 \times 10^{-4} \text{ M}$ (40 ppm); $[\text{NaOMe}] = 1.6 \times 10^{-3}$; $\text{L/Pd} = 2$; $T = 80 \text{ }^\circ\text{C}$, $[\text{butadiene}]_{\text{initial}} = 1.0 \text{ M}$; reaction time = 2 h.

The formation of phosphonium cations by attack of free phosphine on the π -allyl palladium complex to generate a triarylphosphonium octadienyl fragment is analogous to formation of 1-methoxy-2,7-octadiene, **1**, by attack of methoxide (or methanol) on the same complex, in the mechanism proposed by Beller [10]. This phosphonium cation can react with methoxide to form a five-coordinate phosphorane, which itself can then react with methoxide to form phosphine oxide by rupture of one of the phosphorus-carbon bonds of the original phosphonium cation. The P–C bond that is ruptured is known to be that which gives the more stable anion [19]. In this case, the allyl anion is displaced preferentially to the phenyl anion, so the phosphine oxide formed would be expected to be triarylphosphine oxide.

2.3. Electrospray Ionization-Mass Spectrometry

In order to determine why catalysts promoted by more basic phosphine ligands, such as **L8**, showed poorer activity at elevated initial methanol concentrations than those formed from less basic phosphines, such as **L4**, Electrospray Ionization-Mass Spectrometry (ESI-MS) analyses was carried out working telomerization catalyst solutions. The primary goal of ESI-MS analyses was to observe the evolution and course of triarylphosphine ligand degradation throughout the telomerization reaction. The ESI-MS analyses were carried out in the positive ion mode, enabling facile detection of phosphonium cations. Neutral species, such as triarylphosphine oxide, or the phosphorane species, would be expected to be observed as a protonated ($M + 1$) or sodiated cation ($M + 23$).

Spectra of samples run within 15 min after removal from working telomerization reactions using triphenylphosphine-promoted palladium catalysts depict a peak in the ESI-MS spectrum at 371.2 m/z . We assign this to the phosphonium cation (**A**) in Fig. 7. This peak initially grows and then declines in intensity as the reaction progresses. This is consistent with an intermediate species that is both being formed and consumed throughout the telomerization reaction, as we have proposed. Additionally, a peak at 403.2 m/z , corresponding to the $M + 1$ peak of phosphorane (**B**) of Fig. 7, is also observed. This intermediate also initially grows and then declines during the reaction. An alternate structure for this species could be that formed by addition of methanol across one of the double bonds to form another phosphonium salt (species **D** in Fig. 6). We discuss later our rationale for assignment of the 403.2 m/z peak as structure (**B**) and not as (**D**). Finally, a peak at 301.0 m/z , corresponding to the sodium adduct of triphenylphosphine oxide (**C**) of Fig. 7, although not present in the 15 or 30 min spectra, grows

in and persists throughout the remainder of the spectra taken at longer reaction times. This behavior is qualitatively consistent with the expected concentration profiles predicted by the mechanism of Fig. 6.

These data clearly show that phosphonium cations derived from addition of a triphenylphosphine to a C_8 fragment are formed under telomerization reaction conditions. This results in the depletion of triphenylphosphine from the catalyst solution over time. This ligand decomposition occurs concurrently with the loss of palladium observable by ESI-MS throughout the reaction. It also is correlated with the visible appearance of palladium black in working catalyst solutions – the more basic ligands manifest the formation of palladium black earlier than less basic ligands under these conditions. We suggest that the reduction of phosphine ligand concentration by this mechanism is a primary initiator of palladium agglomeration, and ultimately, the complete loss of catalyst activity in working telomerization catalyst solutions.

To distinguish between structures (**B**) and (**D**) of Fig. 6 as the assignment for the 403.2 m/z peak, additional MS/MS experiments were performed. The MS/MS spectrum of this species depicts a fragmentation pattern that is very similar to that observed for species (**A**) of Fig. 7, confirming that the two are closely related. This would be expected for structure (**B**) which could form (**A**) simply by dissociation of methoxide from phosphorus. We believe the fragmentation pattern of structure (**D**) would be significantly different from (**A**) or (**B**), suggesting that (**D**) is not a viable structure for the 403.2 m/z species. However, in the absence of a reference standard for structure (**D**), we have further attempted to distinguish between these possible structures by examining the ESI-MS spectrum of this species in the presence of CD_3OD after it has formed from MeOH. Our rationale is that if the structure is that of (**B**) in Fig. 6, then in the presence of deuterium, the parent ion should also incorporate a D^+ to make the species cationic and give at least some $M + 2$

Table 2
Performance of Selected Triarylphosphines under Relevant Conditions and Concentrations.

Ligand	Chi (χ)	TON	Selectivity to 1 (mol %)
L2	5.6	720	84
L3	10.2	5772	88
L4	12.9	10834	89
L6	16.8	6935	80
L8	2.7	676	86
L9	–8.1	5	6

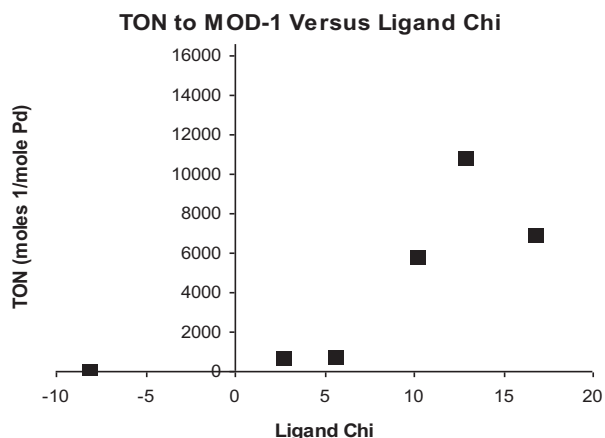


Fig. 5. TON versus Ligand Chi at [methanol] = 12.7 M and [butadiene] = 2.5 M.

peaks in the parent ion. The alternate structure (**D**), inherently being a cation, would be expected to give an unchanged parent ion in the presence of CD_3OD .

The deuterium-labeled methanol experiment was carried out with both triphenylphosphine and tris(2-methoxyphenyl)phosphine-ligated catalysts. Some differences in the data in the two cases were noted. With the triphenylphosphine based catalysts, we noted that the cation $[\text{Ph}_3\text{PCH}_2\text{CH}=\text{CHCH}_2\text{CH}_2\text{CH}_2\text{CH}=\text{CH}_2]^+$ showed the presence of an M^+ cluster of peaks that indicated the presence of one and two substitutions of deuterium for hydrogen in the molecule. This was initially surprising, since, as it is already a cation, no protonation was expected. Review of the literature, however, indicated that exchange of the two octadienyl protons *alpha* to the phosphorus atom is to be expected in the basic catalyst solution which contains sodium methoxide [20].

The species formulated as $[\text{Ph}_3\text{P}(\text{OMe})(\text{CH}_2\text{CH}=\text{CHCH}_2\text{CH}_2\text{CH}_2\text{CH}=\text{CH}_2)]$ (structure (**B**) in Fig. 7; also Supplementary Material Figures I and II) showed an M^+ cluster of peaks that indicated it had incorporated from 1 to 6 deuteriums. We conclude that these arise from incorporation of one or two deuteriums *alpha* to the phosphorus, since this species is derived from the phosphonium cation (structure (**A**) of Fig. 7), with an additional three deuteriums from exchange of CD_3O^- for CH_3O^- bound to phosphorus, and one deuterium to render it cationic. The exchange of alkoxy groups in phosphoranes is known to be facile [21]. This explanation accounts for the observed experimental spectrum. It is not likely that the methyl ether of proposed structure (**D**) of Fig. 6 would exchange

with CD_3O^- under these conditions so this species would be expected to exchange a maximum of 2 deuterons. The observed fragmentation pattern and the deuterium experiment rules out species (**D**) as a possible structure for the 403.2 m/z cluster of peaks.

In the case of tris(2-methoxyphenyl)phosphine, the analogous experiment showed incorporation of deuterium into the *alpha* positions of the octadienyl group of the phosphonium cation, but not into the phosphorane. While we do not have a completely satisfactory explanation of this, we do know that the rate of proton exchange into the *alpha* positions of phosphonium salts becomes slower as the phosphine becomes more basic [22]. If capture of methoxide by the phosphonium in this case is faster than H/D exchange, and is irreversible, this is the result we would expect.

At low methanol concentrations, the performance of tris(2-methoxyphenyl)phosphine, **L8**, is exceptional, giving selectivities of around 95% with good rates. The catalyst activity decays very rapidly, however, particularly under commercial conditions where the methanol concentration is higher. We attribute these effects to the decomposition reaction shown above to occur with triphenylphosphine, and propose that more basic phosphines, such as tris(2-methoxyphenyl)phosphine, would undergo this reaction more rapidly than less basic phosphines. Further, since this decomposition reaction proceeds through a phosphonium cation, and the conversion presumably involves a charge-separated transition state, we suggest that this should be faster in a more polar solvent, such as at high methanol concentration.

To examine these proposals, additional ESI-MS analyses was carried out on tris(2-methoxyphenyl)phosphine-promoted palladium-catalyzed telomerization reaction in comparison to the triphenylphosphine data discussed above. In addition to examining ligand decomposition chemistry, we also hoped to identify differences in the species present under working conditions that might explain the higher linear regiochemistry observed with this ligand.

The ESI-MS spectrum of a solution of tris(2-methoxyphenyl)phosphine (**L8**), acetic acid and $[\text{Pd}(\text{acac})_2]$ in 12.7 M methanol showed the formation of $[\text{Pd}(\text{acac})(\text{P}(\text{C}_6\text{H}_4\text{-2-OMe})_3)_2]^+$ (909.1 m/z) as the predominant product, along with lesser amounts of a mono-phosphine complex, $[\text{Pd}(\text{acac})(\text{P}(\text{C}_6\text{H}_4\text{-2-OMe})_3)]^+$ (557.1 m/z). That triphenylphosphine (**L4**) forms an analogous bis-phosphine complex, but not the corresponding mono-phosphine complex, can be attributed to the larger steric requirements of the tris(2-methoxyphenyl)phosphine (**L8**) compared to triphenylphosphine, which destabilizes the bis-phosphine complex relative to the mono-phosphine complex. There is little change in the spectrum upon addition of sodium methoxide, with only low concentrations of additional palladium-containing species being formed. There are,

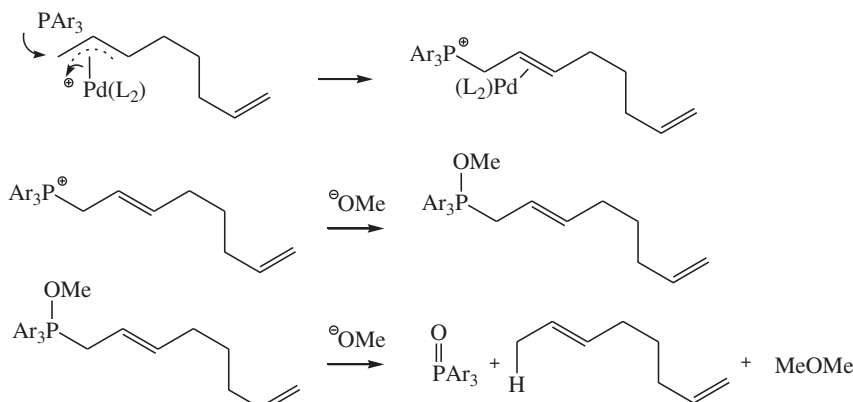


Fig. 6. Proposed mechanism for the formation of phosphonium cation, and subsequent solvolysis to phosphine oxide.

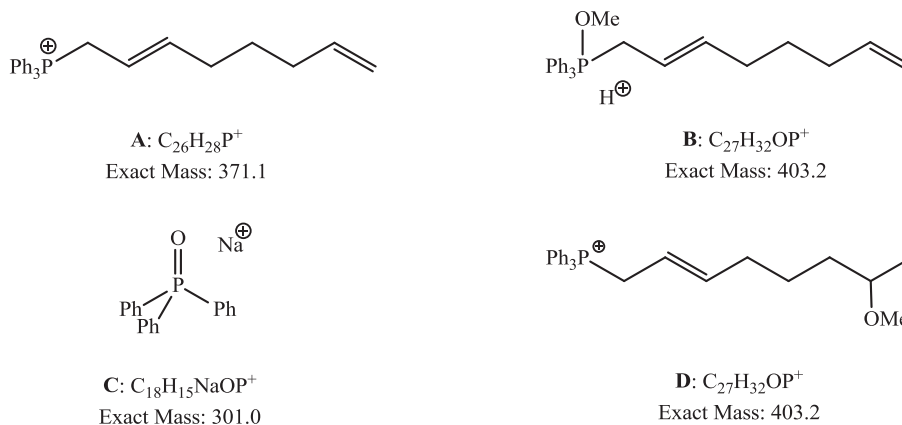


Fig. 7. Possible decomposition products of triphenylphosphine in telomerization catalyst solutions.

however, significant changes in the spectrum of the reaction solution taken 15 min after the addition of butadiene. Although some $[Pd(acac)(P(C_6H_4-2-OMe)_3)_2]^+$ remains, and the formation of some $[Pd(CH_2CH=CHCH_2CH_2CH_2CH=CH_2)(P(C_6H_4-2-OMe)_3)]^+$ is observed, analogous to the complex seen in the triphenylphosphine-promoted catalyst, the intensity of the peaks from these palladium-containing complexes is very low, suggesting that most of the palladium has lost its supporting ligands and is no longer observable in the ESI-MS experiment. The predominant feature in this 15 min spectrum is an ion corresponding to $[(C_6H_4-2-OMe)_3P(CH_2CH=CHCH_2CH_2CH_2CH=CH_2)]^+$ (461.2 m/z), the phosphonium cation corresponding to structure (A) of Fig. 7. After 30 min and thereafter, essentially no palladium complexes are seen in the spectra. The peaks corresponding to $[(C_6H_4-2-OMe)_3PCH_2CH=CHCH_2CH_2CH_2CH=CH_2]^+$ remain, while a new peak, corresponding to species (B) of Fig. 7, grows in.

The data presented above is consistent with rapid formation of a phosphonium salt of the tris(*o*-methoxyphenyl)phosphine very early in the telomerization reaction, with the resulting loss of palladium from solution. This is also consistent with the short lifetime of this catalyst system under telomerization conditions in concentrated methanol solution. We have not yet examined the effect of methanol concentration on the rate of phosphine ligand degradation. We predict that this rate would be significantly lower

at lower MeOH concentration since these catalysts retain activity longer under such conditions.

These data clearly show that the more basic ligand undergoes the same decomposition reaction as triphenylphosphine, but at a much more rapid rate. This observation also suggests that the loss of ligand in telomerization catalyst solutions correlates with loss of catalytic activity, loss of observable palladium in the positive ion ESI-MS spectrum, and the appearance of palladium black in the working catalyst solutions. Fig. 8 shows the evolution of the ESI-MS spectra of the triphenylphosphine and tris(*o*-methoxyphenyl)phosphine-ligated catalysts with time. It clearly demonstrates that the more basic ligand **L8** decomposes more rapidly than triphenylphosphine, which coincides with a loss of ESI-MS detectable palladium.

2.4. Design, synthesis and evaluation of new ligands

The correlations of increased intrinsic activity and selectivity, and of decreased stability, with increasing ligand basicity means that the most basic ligands are unsuitable for commercial use. The remainder of the work reported here focuses on efforts to capture the high selectivity achieved by ligands possessing the *o*-methoxyphenyl substitution motif, by combining it with increased ligand stability. Our approach to this goal was to moderate the phosphine basicity,

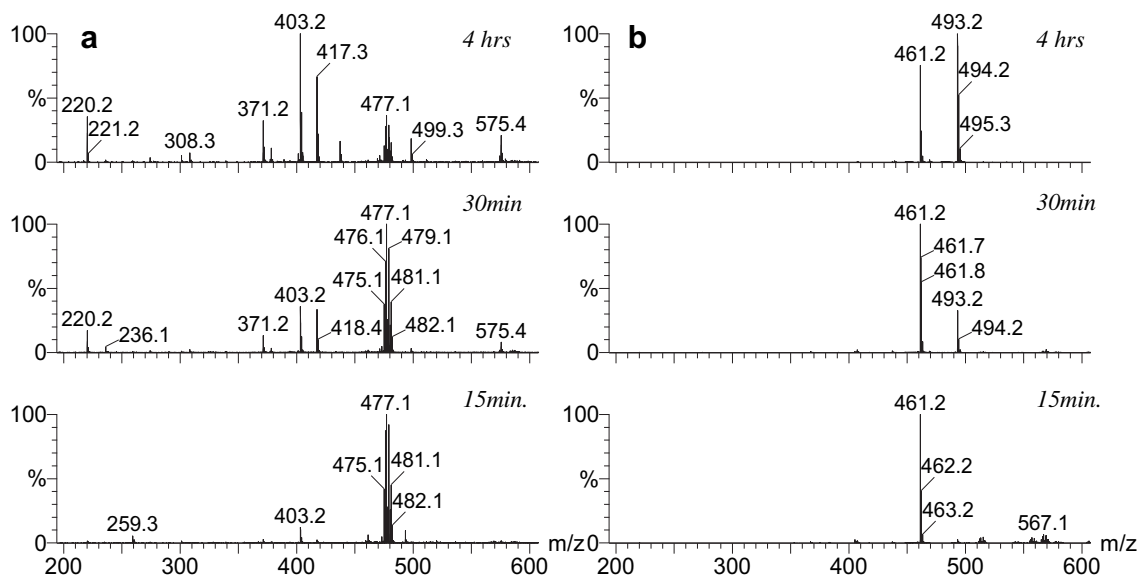


Fig. 8. ESI-MS Spectra (200–600 amu) focusing on the degradation products from working (a) triphenylphosphine and (b) tris(*o*-methoxyphenyl) phosphine catalyst solutions as a function of time.

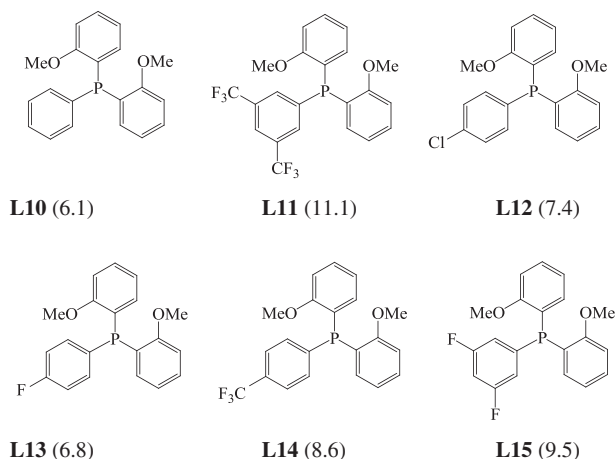


Fig. 9. Bis-*o*-alkoxy substituted aryl phosphines evaluated in this study. The estimated ligand Chi values are shown in parentheses.

e.g., by substituting an arene ring with electron-withdrawing groups. We anticipated that this might slow the decomposition reaction sufficiently to allow such ligands to survive long enough to achieve commercial productivities, while maintaining improved selectivities compared to triphenylphosphine. While *o*-methoxyaryl phosphine ligands used as promoters for telomerization reactions of biomass-derived alcohols and polyols has been reported earlier [23], the incorporation of additional electron-withdrawing groups to improve performance and catalyst stability has not been reported. The synthetic approach taken described here focuses on moderating the basicity of one aryl ring while maintaining the *o*-methoxy substitution of the remaining two aryl rings (Fig. 3). Ligands which were examined to test this hypothesis are shown in Fig. 9, along with the estimated Tolman Chi values in parentheses.

2.5. Ligand synthesis and characterization

The synthesis of ligands **L11**, **L12**, and **L13**, was accomplished by reacting the commercially available starting material chlorobis(2-methoxyphenyl)phosphine with the appropriate Grignard reagent. The synthesis of ligand **L14** was accomplished by performing a lithium-halogen exchange by reacting *n*-BuLi with the precursor 1-bromo-4-(trifluoromethyl)benzene. The *in-situ* generated 1-lithio-4-(trifluoromethyl)benzene was then reacted with chlorobis(2-methoxyphenyl)phosphine to produce the desired product. While the crude yields were generally high, some loss occurred during the

multiple recrystallizations required to remove residual color and obtain highly pure product. The ^{31}P and ^{13}C NMR spectra of the products **L10**–**L15** are consistent with the proposed structures. The ^{31}P NMR analysis of the phosphorus-based ligands showed that the chemical shifts range from -26 to -21 ppm. Spectra of ligands **L11**, **L13**, and **L14** are complex due to the splitting of some ^{13}C resonances by phosphorus and fluorine.

The χ parameters of each ligand included in this study are shown in Fig. 9. These values were estimated using published substituent electronic contributions for phosphine ligands. In the case of ligand **L10**, the electronic contribution of each *m*-CF $_3$ substituent is not reported. In order to estimate the electronic effect of this substitution, the contribution of a *p*-CF $_3$ substituent and related substituents was used to assign this Chi value [24]. By maintaining the bis(2-methoxyphenyl)phosphine framework and varying the donor–acceptor properties of each phosphine ligand by changing the substituents only in the *meta*- and *para*-positions of the third aryl group, the steric differences between these ligands was expected to be small so that performance differences within this subset of phosphine ligands (**L9**–**L15**) were essentially electronic in nature.

2.6. Catalyst screening

The catalytic performance of these new ligands was monitored with time as a function of initial MeOH concentration (12.7 and 5.1 M) at 90 °C by sampling at 30 min, 1 h, 2 h, and 4 h. Details of these experiments can be found in the experimental section. The performance data of palladium catalysts promoted by these ligands is collected in Table 3.

The resulting time series plots are shown in Fig. 9. Excellent selectivities to MOD-1 are achieved by each of the new catalysts compared to that of incumbent ligand **L4**, triphenylphosphine, at each of the MeOH concentrations examined. At a methanol concentration of 5.1 M, the selectivity to MOD-1 observed by the incumbent triphenylphosphine system was 77.9% after 4 h. Under the same conditions, the selectivities of the catalysts derived from the bis(2-methoxyphenyl)phosphine based ligands ranged from 88.0 to 94.9%. At the higher methanol concentration of 12.7 M, the selectivity improvements are less significant, yet the best bis(2-methoxyphenyl)phosphine ligands, **L8** and **L9**, continue to demonstrate improved MOD-1 selectivities of 95.1 and 94.8% respectively, compared to 89.6% for **L4**.

The most striking features of the graphs shown in Fig. 10 are the early flattening of some of the TON versus time curves, which we equate with catalyst death. The plots of reactions carried out in 5.1 M methanol concentration clearly show that **L11**, the least basic ligand, becomes inactive within the first 30 min of the reaction, and

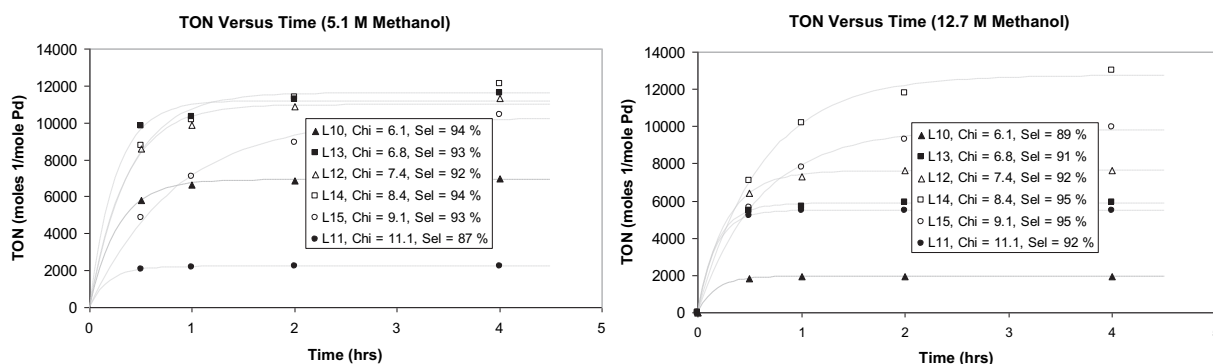


Fig. 10. Performance of the new ligand-promoted palladium catalysts with time at 12.7 M methanol, 5.1 M methanol. $[\text{Pd}] = 8.8 \times 10^{-5}$ M (11 ppmw), $[\text{NaOMe}] = 3.2 \times 10^{-4}$, $\text{L}/\text{Pd} = 2$, $T = 90$ °C, $[\text{butadiene}]_{\text{initial}} = 2.5$ M, reaction time = 2 h. Maximum TON = 16,600.

Table 3
TON (mol **1**/mol Pd) of Selected Bis(2-methoxyphenyl)arylphosphine-Promoted Palladium Catalysts in Butadiene Telomerization with Time and Initial Methanol Concentration.

		Ligand (Tolman Chi Value)						
		Time (hr)	L10 (6.1)	L13 (6.8)	L12 (7.4)	L14 (8.4)	L15 (9.1)	L11 (11.1)
Methanol = 12.7 M	0		0	0	0	0	0	0
	0.5		1831	5478	6440	7094	5653	5174
	1		1940	5682	7283	10169	7814	5470
	2		1924	5924	7654	11779	9273	5490
	4		1949 (89)	5922 (91)	7663 (92)	13022 (95)	9967 (95)	5487 (92)
Methanol = 5.1 M	0		0	0	0	0	0	0
	0.5		5808	9811	8588	8731	4834	2062
	1		6659	10295	9845	10158	7086	2200
	2		6881	11278	10886	11356	8926	2212
	4		6974 (94)	11574 (93)	11305 (92)	12079 (94)	10405 (93)	2206 (87)

Chi values are in parentheses following the ligand label.

Values in parentheses at 4 h are the final selectivity to **1** in mol %.

L10, the most basic ligand, after about 1 h. Ligands **L13**, **L12** and **L14** have very similar profiles, and appear to achieve maximum TON productivity between one and 2 h **L15** remains active for the entire 4 h reaction time. In 12.7 M methanol, catalysts promoted by **L10**, **L13**, and **L11** appear to lose all activity in the first 30 min, **L12** somewhat later in the first hour, while **L14** and **L15** retain activity into the second or third hour of the reactions. Although we do not have a complete understanding of the factors determining the form of these TON versus time plots, we suggest that the anaerobic decomposition reaction described above, coupled with the differential binding of the ligands to the palladium catalyst throughout the catalytic telomerization cycle, likely plays an important role.

Fig. 11 shows the activity of the ligand-stabilized catalysts, expressed as TONs achieved after 4 h reactions at initial [MeOH] = 12.7 and 5.1 M and initial [butadiene] = 2.5 M as a function of ligand basicity. As can be seen, the least basic ligand **L11** with a Chi value of 11.1, gives only moderate productivity to **1** over the 4 h reaction period. As the ligand basicity increases, first to a Chi value of 8.6 for **L14**, the TON performance of each catalyst system steadily improves. **L14** appears to perform close to the optimum for this class of bis(2-methoxyphenyl)phosphine ligands where the effects of increased activity and decreased stability with ligand basicity compete to give a performance optimum in the range of Chi \approx 8–9. As the ligand basicity is further increased progressing through ligands **L10**, **L13**, and **L12**, the primary factor governing the TON performance

of the resulting catalyst systems appears to be ligand instability, as a steady decline in the TON performance over the 4 h period is observed even though initial rates may be high. This is also supported by the visual observation of earlier and increasing amounts of palladium black precipitation during the course of the runs as the ligand basicity is increased. As expected (Fig. 6), these more basic ligands (**L10**, **L13**, and **L12**) perform better at lower methanol concentrations, but experience a decline in performance as the methanol concentrations reach 12.7 M. The selectivities to **1** of the highest productivity ligand-promoted catalysts, which use **L14** and **L15**, are also very high under both methanol concentrations. Consequently, catalysts based on this ligand class, particularly **L14**, are considered viable candidates for commercial use under a wider variety of process conditions.

3. Conclusions

We have shown that catalyst systems containing basic triaryl-based phosphines, especially *ortho*-methoxy-substituted triarylphosphines at low methanol concentration, give enhanced catalyst performance in the process catalytically telomerizing two equivalents of 1,3-butadiene to 1-methoxy-2,7-octadiene (MOD-1) in methanol. Improvements are seen in both selectivity and activity. At higher methanol concentrations, however, competing effects of increased activity/selectivity and decreased stability with increasing ligand basicity generate a performance optimum at moderate ligand basicity under these more commercially-relevant conditions. Loss of ligand from telomerization solutions was shown to be a result of alkylation by an octadienyl group, forming phosphonium salts, phosphoranes, and in one case, phosphine oxide, which were observed by ESI-MS. Concurrent loss of ESI-MS-observable palladium was also demonstrated. These observations lead us to the suggestion that phosphine decomposition is the triggering event that causes catalyst deactivation in phosphine-promoted telomerization catalysts. Improved performance was achieved by moderating the phosphine ligand basicity, e.g., by substituting one arene ring with electron-withdrawing groups, while maintaining the *ortho*-methoxyphenyl structural motif of the remaining two aryl rings.

4. Experimental

4.1. Preparation of solvents and reagents

All solvents and reagents were handled and purified (if applicable) in a glovebox under nitrogen. Anhydrous methylcyclohexane (MCH) and methanol (CH₃OH) purchased from Aldrich were purified further by flowing each solvent through a short column of activated

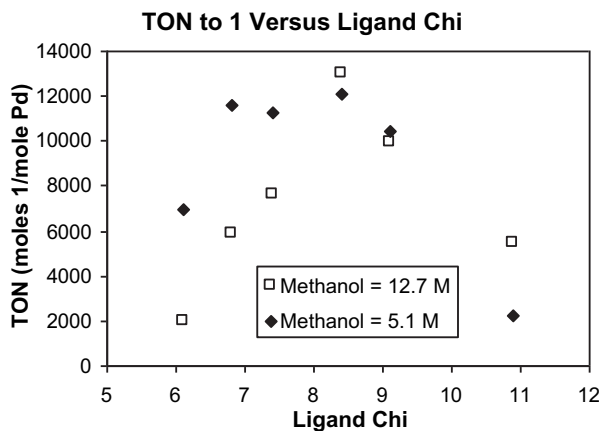


Fig. 11. Plot of Ligand Chi versus TON (at 4 h reaction time) of the new ligand set demonstrating the effects of increased activity and decreased stability with ligand basicity competing to give a ligand optimum. Maximum TON = 16,600 possible, 90 °C, [MeOH] = 12.7 M or 5.1 M, L/Pd = 2.

alumina and a layer of silica gel to keep the alumina fines from coming through the filter. Dibutyl ether, which is used as an internal standard for gas chromatography analysis, was purchased from Aldrich, and prepared by first stirring it over sodium (Na)/potassium (K) alloy overnight and then flowing it through a short column of activated alumina and a layer of silica gel to keep the alumina fines from coming through the filter. Chlorobis(2-methoxyphenyl)phosphine was purchased from Alpha Aesar and used as is (3,5-Bis(trifluoromethyl)phenyl) magnesium bromide, (4-chlorophenyl) magnesium bromide, (4-fluorophenyl)magnesium bromide, (3,5-difluorophenyl)magnesium bromide, **L10**, and 1-bromo-4-(trifluoromethyl)benzene, as well as all other reagents, were used as purchased from Aldrich unless otherwise noted.

4.1.1. Catalytic telomerization screening

Precatalyst stock solutions were prepared by dissolving Pd(acac)₂ (0.0294 g, 0.0966 mmol), phosphine (0.1932 mmol), and acetic acid (0.0966 mmol) in 0.50 mL of 0.193 M HOAc in CH₃OH in MeOH to give a total volume of 50.00 mL. The two equivalents of acetic acid are used as a stabilizing additive in the plant catalyst preparation maintained in this study to best mimic commercial catalyst handling. Into an open Fischer-Porter bottle were syringed dibutyl ether, MeOH, methylcyclohexane, the precatalyst stock solution (1.00 mL), and the NaOMe solution. In a typical experiment four reactors are run in parallel with only the methanol concentrations varying (5.1 and 12.7 M) and the initial volume being 25.1 mL. The Fischer-Porter vessel was then attached to a manifold equipped with a pressure gauge and a sampling valve. Approximately 3.5 g (5.5 mL) of 1,3-butadiene was measured into a gas-tight syringe. The butadiene had been previously distilled from the container in which it was received into a Fischer-Porter bottle to remove inhibitor. The 1,3-butadiene was then injected into the reactor *via* the septum with the needle placed just below the surface of the liquid to facilitate dissolution. The initial concentrations of the components are dibutyl ether = 1.17 M, methylcyclohexane = 9.4 M or 0.50 M depending upon 5.1 M or 12.7 M MeOH conditions respectively, [Pd] = 7.7×10^{-5} M, NaOMe = 3.8×10^{-4} M, and 1,3-butadiene = 2.54 M. The reactor was then placed into the preheated oil bath with stirring and allowed to react for a period of 4 h. The reactor was sampled periodically using a gas-tight syringe for gas chromatographic analysis. Gas chromatographic analysis was performed on an HP-6890 gas chromatograph using a DB-1701 column at constant gas flow. Dibutyl ether was employed as internal standard. Response factors were determined using samples of known composition.

4.1.2. Preparation of (3,5-Bis(trifluoromethyl)phenyl)bis(2-methoxyphenyl)phosphine, **L11**

(3,5-Bis(trifluoromethyl)phenyl)magnesium bromide (2.02 mmol, 4.01 mL of a 0.5 M solution in THF) was added dropwise to a solution of chlorobis(2-methoxyphenyl)phosphine (0.515 g, 1.84 mmol) in THF (50 mL) at 0 °C. This mixture was then heated to reflux overnight. After the reaction period the volatiles were removed and the mixture was extracted and filtered using toluene. Removal of the toluene resulted in the isolation of a yellow/brown solid which was extracted using a minimum amount of acetonitrile, filtered, and placed in the freezer (−10 °C) over the weekend during which time the desired product crystallized as a white solid which was isolated by decanting away the solution and drying under vacuum (0.502 g, 59.7%). ¹H NMR (C₆D₆): δ 3.08 (s, 6 H), 6.41 (dd, ³J_{HH} = 7.8 and 4.5 Hz, 2 H), 6.65 (t, ³J_{HH} = 7.5 Hz, 2 H), 6.91 (dt, ³J_{HH} = 6.4 and 1.5 Hz, 2 H), 7.03 (dt, ³J_{HH} = 7.7 and 1.2 Hz, 2 H), 7.67 (s, 1 H), 7.88 (d, ³J_{HH} = 5.7 Hz, 2 H). ¹³C NMR (C₆D₆): 55.2, 110.8, 121.6, 123.6 (d, 14.0 Hz), 125.8, 131.3, 131.7 (d, 6.1 Hz), 133.8 (d, 20.6 Hz), 134.4 (d, 6 Hz), 142.9 (d, 21.2 Hz), 161.7 (d, 14.2 Hz). ³¹P NMR (C₆D₆, externally referenced using H₃PO₄):

δ −21.1. ¹⁹F NMR (C₆D₆, externally referenced using CCl₃F): −63.0. Anal. Calcd for C₂₂H₁₇F₆O₂P: C, 57.65; H, 3.74, found: C, 57.57; H, 3.83. ESI-TOF-MS (Positive Mode) calcd for (M + H)⁺ ion of C₂₂H₁₇F₆O₂P: 459.095 amu, found 459.095 amu.

4.1.3. Preparation of (4-Chlorophenyl)bis(2-methoxyphenyl)phosphine, **L12**

(4-Chlorophenyl)magnesium bromide (2.51 mmol, 2.51 mL of a 1.0 M solution in diethylether) was added dropwise to a solution of chlorobis(2-methoxyphenyl)phosphine (0.640 g, 2.28 mmol) in THF (50 mL) at 0 °C. This mixture was then heated to reflux overnight. After the reaction period the volatiles were removed and the mixture was extracted and filtered using toluene. Removal of the toluene resulted in the isolation of a solid which was then dissolved in warm acetonitrile (20 mL), filtered, and placed in the freezer (−10 °C) overnight during which time a white crystalline solid formed. This material was isolated by decanting the liquid away and then dried under vacuum resulting in the isolation of the desired product (0.626 g, 77.0%). ¹H NMR (C₆D₆): δ 3.17 (s, 6 H), 6.49 (dd, ³J_{HH} = 8.2 and 4.5 Hz, 2 H), 6.75 (t, ³J_{HH} = 7.4 Hz, 2 H), 6.93–7.29 (m, 8 H). ¹³C NMR (C₆D₆): 55.3, 110.6, 121.4, 125.8 (d, 15.0 Hz), 130.4, 134.1, 134.9, 135.9 (d, 21.8 Hz), 136.4 (d, 14.2 Hz), 161.8 (d, 16.5 Hz). ³¹P NMR (C₆D₆, externally referenced using H₃PO₄): δ −26.1. Anal. Calcd for C₂₀H₁₈ClO₂P: C, 67.33; H, 5.09, found: C, 66.35; H, 5.18. ESI-TOF-MS (Positive Mode) calcd for (M + H)⁺ ion of C₂₀H₁₈ClO₂P: 357.081 amu, found 357.081 amu.

4.1.4. Preparation of (4-Fluorophenyl)bis(2-methoxyphenyl)phosphine, **L13**

(4-Fluorophenyl)magnesium bromide (3.14 mmol, 1.57 mL of a 2.0 M solution in diethylether) was added dropwise to a solution of chlorobis(2-methoxyphenyl)phosphine (0.880 g, 2.85 mmol) in THF (50 mL) at 0 °C. This mixture was then heated to reflux overnight. After the reaction period the volatiles were removed and the residue was extracted and filtered using toluene. Removal of the toluene resulted in the isolation of a yellow/brown solid which was extracted using a minimum amount of acetonitrile, filtered and placed in the freezer (−10 °C) overnight during which time the desired product crystallized as a white solid which was isolated by decanting away the solution and drying under vacuum (0.560 g, 54.5%). ¹H NMR (C₆D₆): δ 3.18 (s, 6 H), 6.50 (dd, ³J_{HH} = 9.0 and 6.0 Hz, 2 H), 6.68–6.81 (m, 4 H), 6.93–6.99 (m, 2 H), 7.08–7.15 (m, 2 H), 7.26–7.35 (m, 2 H). ¹³C NMR (C₆D₆): 55.2, 110.5, 115.5 (d, 7.6 Hz), 115.8 (d, 7.7 Hz), 121.3, 130.3, 134.0, 136.4 (d, 7.6 Hz), 136.7 (d, 8.4 Hz), 161.7 (d, 16.0 Hz), 165.3. ³¹P NMR (C₆D₆, externally referenced using H₃PO₄): δ −26.0. ¹⁹F NMR (C₆D₆, externally referenced using CCl₃F): −113.5. Anal. Calcd for C₂₀H₁₈FO₂P: C, 70.58; H, 5.33, found: C, 69.55; H, 5.51. ESI-TOF-MS (Positive Mode) calcd for (M + H)⁺ ion of C₂₀H₁₈FO₂P: 341.111 amu, found 341.111 amu.

4.1.5. Preparation of Bis(2-methoxyphenyl)(4-(trifluoromethyl)phenyl)phosphine, **L14**

1-Bromo-4-(trifluoromethyl)benzene (0.593 g, 2.63 mmol) was stirred in diethylether (30 mL) at 0 °C as *n*-BuLi (2.63 mmol, 1.32 mL of a 2.0 M solution in cyclohexane) was added dropwise. This mixture was allowed to stir for an additional hour. Chlorobis(2-methoxyphenyl)phosphine (0.739 g, 2.63 mmol) was then added as a solid and the mixture allowed to stir for an additional 4 h at room temperature. After the reaction period the volatiles were removed and the residue was dissolved in benzene and filtered to remove the salts. Removal of the volatiles from the filtrate resulted in the isolation of a yellow residue which was dissolved in a minimum amount of acetonitrile, filtered, and placed in the glovebox freezer (−10 °C) overnight during which time crystals precipitated which were isolated by decanting off the liquid and drying under vacuum.

This recrystallization process was performed three times resulting in the isolation of the desired product as a white microcrystalline solid (0.419 g, 49.3%). ^1H NMR (C_6D_6): δ 3.16 (s, 6 H), 6.47–6.52 (m, 2 H), 6.71–6.77 (m, 2 H), 6.90–6.95 (m, 2 H), 7.08–7.15 (m, 2 H), 7.21–7.25 (m, 2 H), 7.31–7.37 (m, 2 H). ^{13}C NMR (C_6D_6): 55.2, 110.6, 121.4, 125.1 (m), 130.7, 134.23, 134.25, 134.4, 134.7, 143.4, 161.8 (d, 15.7 Hz). ^{31}P NMR (C_6D_6 , externally referenced using H_3PO_4): δ –24.6. ^{19}F NMR (C_6D_6 , externally referenced using CCl_3F): –62.7. Anal. Calcd for $\text{C}_{21}\text{H}_{18}\text{F}_3\text{O}_2\text{P}$: C, 64.62; H, 4.65, found: C, 64.85; H, 4.68. ESI-TOF-MS (Positive Mode) calcd for $(\text{M} + \text{H})^+$ ion of $\text{C}_{21}\text{H}_{18}\text{F}_3\text{O}_2\text{P}$: 391.107 amu, found 391.108 amu.

4.1.6. Preparation of Bis(2-methoxyphenyl)(3,5-difluorophenyl)phosphine, **L15**

Chlorobis(2-methoxyphenyl)phosphine (0.666 g, 2.37 mmol) was stirred in diethylether (30 mL) at 0 °C as (3,5-difluorophenyl)magnesium bromide (2.37 mmol, 4.74 mL of a 0.5 M solution in diethylether) was added dropwise. This mixture was allowed to stir overnight at room temperature. After the reaction period the volatiles were removed and the residue was dissolved in benzene and filtered to remove the salts. Removal of the volatiles from the filtrate resulted in the isolation of a dark yellow residue which was dissolved in a minimum amount of acetonitrile, filtered, and placed in the glovebox freezer (–10 °C) overnight during which time crystals precipitated which were isolated by decanting off the liquid and drying under vacuum. This recrystallization process was repeated until the product was isolated as a white microcrystalline solid (0.350 g, 41.2%). ^1H NMR (C_6D_6): δ 3.14 (s, 6 H), 6.39–6.49 (m, 2 H), 6.67–6.75 (m, 2 H), 6.90–7.17 (m, 7 H). ^{13}C NMR (C_6D_6): 55.3, 104.0 (t, 25 Hz), 110.7, 116.5 (m), 121.5, 124.7 (d, 14.2 Hz), 130.8, 134.1 (d, 2.2 Hz), 140.7, 161.8 (d, 16.0 Hz), 165.0 (m). ^{31}P NMR (C_6D_6 , externally referenced using H_3PO_4): δ –22.7. ^{19}F NMR (C_6D_6 , externally referenced using CCl_3F): –110.3 (m). Anal. Calcd for $\text{C}_{20}\text{H}_{17}\text{F}_2\text{O}_2\text{P}$: C, 67.04; H, 4.78, found: C, 66.61; H, 4.72. ESI-TOF-MS (Positive Mode) calcd for $(\text{M} + \text{H})^+$ ion of $\text{C}_{20}\text{H}_{17}\text{F}_2\text{O}_2\text{P}$: 359.101 amu, found 359.102 amu.

4.1.7. ESI-MS analyses

All samples were transferred in Hamilton Gas-Tight Syringes to a drybox adjacent to the mass spectrometer. The syringes were subsequently removed from the drybox and infused directly into a syringe needle adapter union on the Z-spray Electrospray probe of a Waters-Q-ToF II Mass Spectrometer. This allowed the sample to be manually infused from the syringe to the ESI probe without any intervening tubing. In order to avoid carry-over between different time-point injections, the probe was cleaned by infusing dry methanol after each analysis. The Time of Flight (ToF) analyzer was calibrated prior to analysis using a calibrant solution (2 $\mu\text{g}/\mu\text{L}$ NaI/0.05 $\mu\text{g}/\mu\text{L}$ CsI in 1/1 isopropanol/water) at a flow rate of 10 $\mu\text{L}/\text{min}$. Data acquisition was performed with a cycle time of 1 scan/sec (scan acquisition time: 0.88 s; interscan delay: 0.1 s) in the MS mode. The infusion rate was approximately 20–50 $\mu\text{L}/\text{min}$. The following mass spectral conditions were utilized: MCP Detector: 2150 V; Resolution: 9000; Data Acquisition Mode: Continuum Positive Ion Mode; Mass Scan: 50–2100 amu; Capillary Voltage: 2500 V; Cone Voltage: 20 V; Source Temperature: 110 °C; Desolvation Temperature: 300 °C; Desolvation Gas: Nitrogen at 60 psig. In MS/MS mode, fragmentation of each component was carried out separately with collision energies set to 25 V, 30 V, 35 V and 40 V. The instrument was scanned at 0.5 scan per seconds and the mass range was set to 100–1900 m/z .

Conditions: $[\text{Pd}] = 7.7 \times 10^{-5}$ M (10.9 ppm), L/Pd = 2 mol/mol, $[\text{butadiene}]_{\text{initial}} = 2.5$ M, $[\text{MeOH}]_{\text{initial}} = 12.7$ M, $T = 90$ °C, reaction time = 2 h. Methylcyclohexane was added to bring the total reaction volume to the same value. Reactions were conducted in sealed Fischer-Porter tubes immersed in a constant temperature bath. Experimental details are reported in the experimental section. Maximum TON for 100% yield of **1** is ~16,600.

Appendix. Supplementary data

Supplementary data associated with the article can be found in online version, at doi:10.1016/j.jorganchem.2011.02.007.

References

- [1] J.M. Takacs, in: E.W. Abel, G. Stone, G. Wilkinson, Series Eds, L.S. Hegadus, Vol. Ed (Eds.), *Comprehensive Organometallic Chemistry II*, vol. 12, Chapt. 8.1, Elsevier Science Ltd, Oxford, New York, Tokyo, 1995, p. 785.
- [2] (a) E.J. Smutny, *J. Am. Chem. Soc.* 89 (1967) 6793; (b) S. Takahashi, T. Shibano, N. Hagihara, *Tetrahedron Lett.* 8 (1967) 2451.
- [3] A. Behr, M. Becker, T. Beckmann, L. Johnen, J. Leschinski, S. Reyer, *Angew. Chem. Int. Ed.* 48 (2009) 3598.
- [4] (a) B.J. Schaart, H.L. Pelt, G.B. Jacobsen, *Continuous Process for the Telomerization of Conjugated Dienes U. S. Patent 5,254,782* (October 19, 1973); (b) B. Estrine, S. Bouquillon, F. Hénin, J. Muzart, *Eur. J. Org. Chem.* (2004) 2914–2922; (c) M. Basato, L. Crociani, F. Benvenuti, A.M.R. Galletti, G. Sbrana, *J. Mol. Cat. A: Chem.* 145 (1999) 313; (d) C.L. Edwards, *Process for Producing Detergent Molecules Comprising an Ether Linkage from Butadiene U. S. Patent 7,141,539* (November 28, 2006).
- [5] E. Singer, R. Landgraf, D.J. Slamon, D. Eisenberg, *Process for Production of Ethers U. S. Patent 7,314,916* (January 1, 2008).
- [6] R. Jackstell, S. Harkal, H. Jiao, A. Spannenberg, C. Borgmann, D. Röttger, F. Nierlich, M. Elliot, S. Niven, K. Cavell, O. Navarro, M.S. Viciu, S.P. Nolan, M. Beller, *Chem. Eur. J.* 10 (2004) 3891.
- [7] F. Benvenuti, C. Carlini, M. Lami, M. Marchionna, R. Patrini, A.M.R. Galletti, G. Sbrana, *J. Mol. Cat. A: Chem.* 144 (1999) 27.
- [8] W. Keim, in: G.N. Schrauzer (Ed.), *Transition Metals in Homogeneous Catalysis*, Marcel Dekker, New York, 1971.
- [9] (a) P.W. Jolly, R. Mynott, B. Rasper, K.-P. Schick, *Organometallics* 5 (1986) 473; (b) R. Benn, P.W. Jolly, R. Mynott, B. Rasper, G. Schenker, K.-P. Schick, G. Schroth, *Organometallics* 4 (1985) 1945.
- [10] F. Vollmüller, J. Krause, S. Klein, W. Mägerlein, M. Beller, *Eur. J. Inorg. Chem.* (2000) 1825.
- [11] M.J.-L. Tschan, E.J. Garcia-Suarez, Z. Freixa, H. Launay, H. Hagen, J. Benet-Buchholz, P.W.N.M. van Leeuwen, *J. Am. Chem. Soc.* 132 (2010) 6463.
- [12] D. Beigzadeh, *Macro. React. Eng.* 1 (2007) 331.
- [13] (a) C.A. Tolman, *Chem. Rev.* 77 (1977) 313; (b) F. Benvenuti, C. Carlini, M. Lami, M. Marchionna, R. Patrini, A.M.R. Galletti, G. Sbrana, *J. Mol. Cat. A: Chem.* 144 (1999) 27.
- [14] S.J. Chen, K.R. Dunbar, *Inorg. Chem.* 29 (1990) 588.
- [15] US Patent 7,041,619, May 9, 2006, assigned to Kuraray.
- [16] S.M. Maddock, M.G. Finn, *Organometallics* 19 (2000) 2684.
- [17] K.L. Granberg, J.-E. Backwall, *J. Am. Chem. Soc.* 114 (1992) 6858.
- [18] M. Grayson, P.T. Keough, *J. Am. Chem. Soc.* 82 (1960) 3919.
- [19] J.R. Corfield, S. Trippett, *J. Chem. Soc. D: Chem. Comm.* 19 (1970) 1267.
- [20] (a) S.E. Cremer, R.J. Chhorvat, *Tetrahedron Lett.* 4 (1966) 419; (b) M.-C. Tseng, H.-C. Kan, Y.-H. Chu, *Tetrahedron Lett.* 48 (2007) 9085.
- [21] B.C. Chang, W.E. Conrad, D.B. Denney, D.Z. Denny, R. Edelman, R.L. Powell, D.W. White, *J. Am. Chem. Soc.* 93 (1971) 4004.
- [22] (a) S.E. Cremer, R.J. Chhorvat, *Tet. Lett.* 4 (1966) 419–421; (b) C. M.-Tseng, H.-C. Kan, Y.-H. Chu, *Tet. Lett.* 48 (2007) 9085–9089.
- [23] (a) P.J.C. Hausoul, P.C.A. Bruijninx, R.J.M. Klein Gebbink, B.M. Weckhuysen, *Chem. Sus. Chem.* 2 (2009) 855; (b) R. Palkovits, I. Nieddu, C.A. Kruihof, R.J.M. Klein Gebbink, B.M. Weckhuysen, *Chem. Eur. J.* 14 (2008) 8995; (c) R. Palkovits, I. Nieddu, R.J.M. Klein Gebbink, B.M. Weckhuysen, *Chem. Sus. Chem.* 1 (2008) 193; (d) R. Palkovits, A.N. Parvulescu, P.J.C. Hausoul, C.A. Kruihof, R.J.M. Klein Gebbink, B.M. Weckhuysen, *Green Chem.* 11 (2009) 1155.
- [24] (a) M.R. Wilson, H. Liu, A. Prock, W.P. Giering, *Organometallics* 12 (1993) 2044; (b) A. Fernandez, C. Reyes, M.R. Wilson, D.C. Woska, A. Prock, W.P. Giering, *Organometallics* 16 (1997) 342.